Solid-State Electronics 54 (2010) 777–780

Contents lists available at ScienceDirect

Solid-State Electronics

journal homepage: www.elsevier.com/locate/sse

Direct measurement of electron beam induced currents in p-type silicon

Myung-Geun Han [a,c,*], Yimei Zhu [c], Katsuhiro Sasaki [b], Takeharu Kato [a], Craig A.J. Fisher [a], Tsukasa Hirayama [a]

[a] Nanostructures Research Laboratory, Japan Fine Ceramics Center, 2-4-1 Mutsuno, Atsuta-ku, Nagoya 456-8587, Japan
[b] Department of Quantum Engineering, Nagoya University, Furo-cho, Chikusa-ku, Nagoya, 464-8603, Japan
[c] Brookhaven National Laboratory, Building 480, Upton, NY 11973, USA

ARTICLE INFO

Article history:
Received 29 October 2009
Accepted 8 March 2010
Available online 8 April 2010

The review of this paper was arranged by Prof. S. Cristoloveanu

Keywords:
Transmission electron microscopy
EBIC
Carrier transport
Semiconductor

ABSTRACT

A new method for measuring electron beam induced currents (EBICs) in p-type silicon using a transmission electron microscope (TEM) with a high-precision tungsten probe is presented. Current–voltage (*I–V*) curves obtained under various electron-beam illumination conditions are found to depend strongly on the current density of the incoming electron beam and the relative distance of the beam from the point of probe contact, consistent with a buildup of excess electrons around the contact. This setup provides a new experimental approach for studying minority carrier transport in semiconductors on the nanometer scale.

Published by Elsevier Ltd.

1. Introduction

Measurement of electron beam induced current (EBIC) has been widely used to study correlations between electronic properties and structural defects in semiconductors [1–6]. Electron–hole pairs (ehps) generated within the interaction volume of the sample by incident electrons can be separated by an internal electric field such as within a p–n junction or a Schottky contact, resulting in a reverse current. To date, EBIC measurement has been mostly performed inside scanning electron microscopes (SEMs) equipped with an electrical stage. The spatial resolution of this method, however, is limited because of the relatively large interaction volumes generated by the primary electrons.

In an effort to confine ehp generation to smaller volumes and thereby improve the spatial resolution, EBIC measurement has also been performed using scanning transmission electron microscopes (STEMs) [3–6]. Although an impinging electron of a few hundred keV typically generates multiple ehps in semiconductors, it has been reported that the EBIC in a 300 nm thick sample is on the order of only a few nA, i.e., less than the incident-beam current itself [1]. This discrepancy has been attributed mainly to the fast carrier recombination at the surfaces of thin specimens, since the higher surface-to-volume ratio means ehps are more likely to recombine while traveling to the collecting junction at the end of the specimen. Electrical contacts between the sample and collecting junction can also cause significant loss of current because of their high resistance.

In this study, we overcome these limitations using a specially designed transmission electron microscope (TEM) holder (Nanofactory Instruments) equipped with a piezo-controlled tungsten probe. This probe has ±2 mm motion range and picometer position control, so that it can be brought into contact with the edge of the sample *in situ* with high precision. This *in situ* probe contact simplifies the overall electrical connection and makes it possible to measure EBICs with little signal loss.

2. Experimental setup

A p-type Si (1 0 0) wafer with dopant concentration 10^{18} cm^{-3} was used as a model semiconducting material. The wafer was first mechanically polished to an electron-transparent thickness (~200 nm) and cleaved in air. The sample was then glued to a half-cut molybdenum washer using silver paste. To avoid surface damage caused by high energy ions, no Ar ion milling was used.

To obtain an even more reliable electrical contact, a thin Pt/Pd film was deposited on the surface of the *W* probe by sputtering. The sample was then attached to the holder and introduced into the TEM (JEM 3000F). *I–V* curves were obtained using the digital multimeter built into the controller system of the holder. The second condenser lens focus and shift coils of the microscope were used to control electron beam diameter and the electron beam

* Corresponding author at: Brookhaven National Laboratory, Building 480, Upton, NY 11973, USA. Tel.: +1 631 344 2391; fax: +1 631 344 4071.
E-mail address: mghan@bnl.gov (M.-G. Han).

0038-1101/$ - see front matter Published by Elsevier Ltd.
doi:10.1016/j.sse.2010.03.008

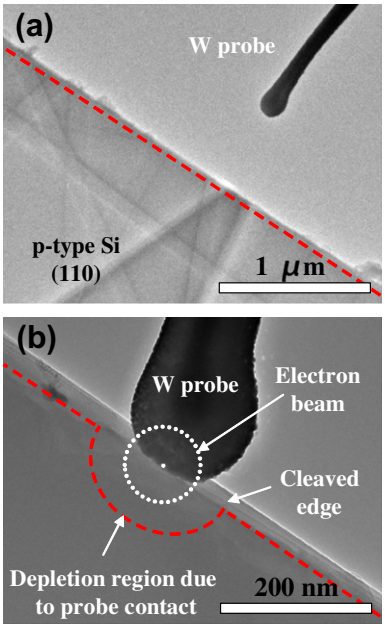

Fig. 1. Bright-field TEM images taken (a) before and (b) after forming a contact. The depletion boundaries are shown as red broken lines. The area illuminated by a 100 nm diameter electron beam centered on the contact is also indicated in (b). (For interpretation of the references to color in this figure legend, the reader is referred to the web version of this article.)

position, respectively. The condenser aperture was not altered during *I–V* curve acquisition to ensure a constant electron beam current. An accelerating voltage of 300 keV was used throughout.

3. Results and discussion

Fig. 1a shows a bright-field TEM image of the p-type Si sample and *W* probe before contact. The sample edge appeared to have a cleaved plane, as shown in Fig. 1b. The *W* probe was brought into contact with the edge of the sample using the piezo-controller, as shown in Fig. 1b. The setup is illustrated schematically in Fig. 2a. The resulting contact area was estimated to be ~100 nm in diameter. After forming an electrical contact, an external bias was applied to the p-type Si sample via a counter-electrode with the *W* probe grounded, as illustrated in Fig. 2a. In this arrangement, the majority carrier (hole) current under forward bias (p-type Si is positive) flows from the counter-electrode side to the *W* probe side of the sample. The contact between the probe and the sample is likely to be the current-limiting factor because of its smaller contact area compared to the counter-electrode.

At all surfaces of the p-type Si, majority carriers (holes) are expected to be depleted due to Fermi-level pinning. If the Fermi level is pinned somewhere near the middle of the bandgap of Si, the depletion width will be about 30 nm from the surface. In Fig. 1a, the boundary of the depletion region (red broken line) is shown before the probe is brought into contact with the sample. It should be noted that not only the edge of the sample but also its top and bottom surfaces are carrier-depleted. Once electrical contact is made, additional band bending due to charge exchange between the *W* probe and the sample may occur, which flattens the Fermi level between them, creating a hemispherical depletion region near the probe contact, as indicated in Fig. 1b. This hemispherical depletion region will expand and shrink in response to the external bias applied across the probe contact.

Fig. 2a shows a schematic side view of the sample in contact with the *W* probe under steady-state electron-beam illumination of two different diameters (d_1 and d_2) and the resulting excess electron profiles in the p-type Si. We assumed a uniform distribution of electron beam intensity and also that local excess electron concentrations are uniform inside the illuminated region and decay exponentially outward from the boundary of the illuminated region by carrier diffusion. Since the illuminating electron beam current is kept constant, the total number of ehps (corresponding to the area under the carrier concentration profiles) generated in the sample will be the same regardless of the beam diameter. Thus, smaller beam diameters result in higher concentrations of excess electrons confined within the hemispherical depletion region. The EBIC is proportional to the total number of excess electrons present within the collecting region, i.e., the combination of the depletion region of diameter Δ and the region within an electron diffusion length, L_n, from the edge of the depletion region. In determining L_n, effects

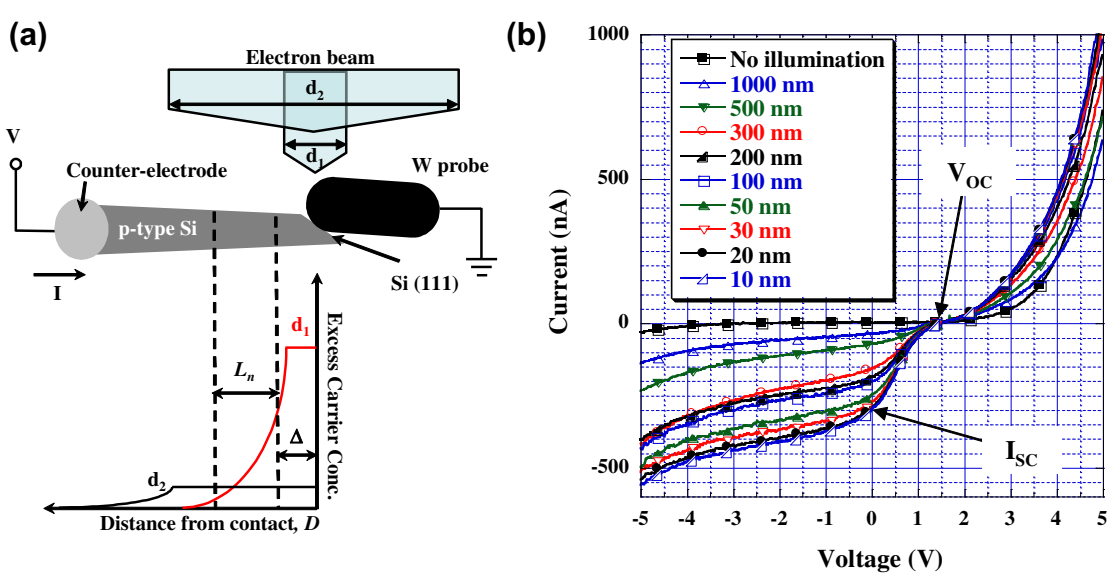

Fig. 2. (a) Schematic side view of the p-type Si sample and *W* probe illuminated by beams of diameter d_1 and d_2, with the resulting excess carrier profiles shown below. Δ is the diameter of the depletion region and L_n is the electron diffusion length. (b) *I–V* curves obtained with various beam diameters ranging from 1000 nm down to 10 nm centered at the contact. The electron gun valve of the microscope was closed to obtain the *I–V* curve for the non-illuminated sample.

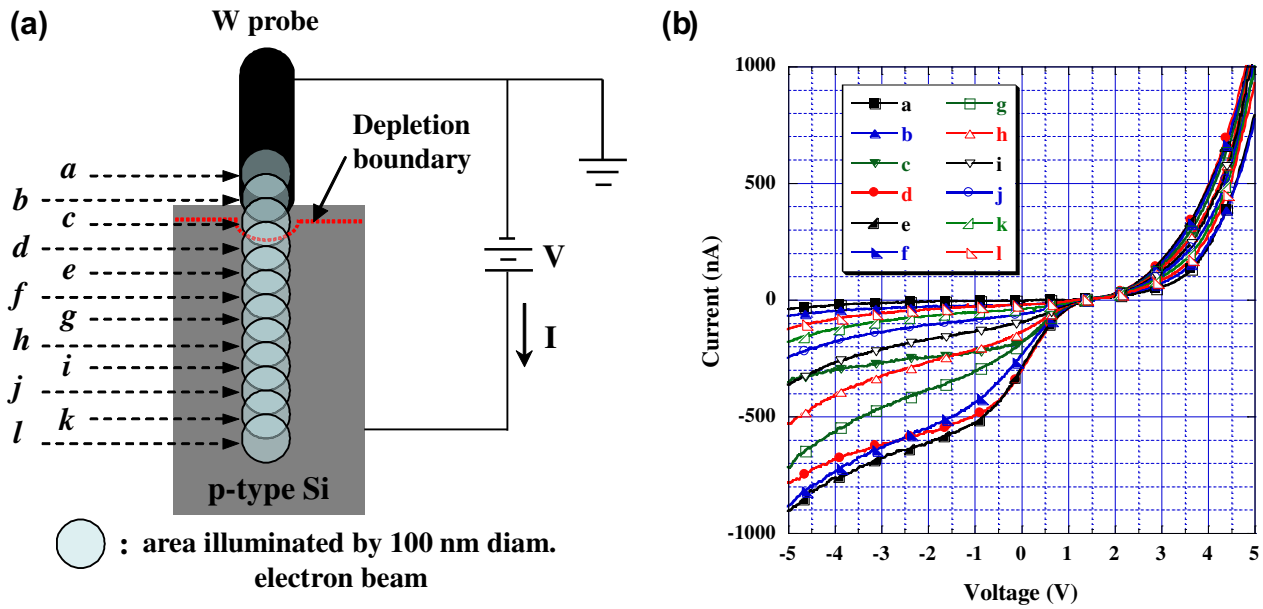

Fig. 3. (a) Schematic showing positions of the 100 nm diameter electron beam during *I–V* measurement. Position *c* corresponds to when the electron beam was centered on the point of probe contact. Beam centers were roughly 50 nm apart. (b) Corresponding *I–V* curves obtained for beam positions in (a).

from carrier deflection by the magnetic field (~2 T) due to excitation of the objective lens have not been taken into account because the carrier diffusion process is driven solely by the carrier concentration gradient.

Fig. 2b shows *I–V* curves obtained from illumination with beams of various diameters, all centered at the position of probe contact. All *I–V* curves are nonlinear due to the rectifying characteristics typical of a metal–semiconductor contact. The reverse current can be seen to dramatically increase with decreasing electron beam diameter; this is because more excess electrons are generated within the collection region, as described above (and illustrated in Fig. 2a). The short-circuit currents, I_{SC}, across the probe contact measured at 0 V also increase with decreasing beam diameter, as shown in Fig. 2b. The slight increase in reverse current with reverse voltage can be explained by the expansion of the depletion region with reverse voltage, resulting in an expansion of the collection region. It is also found that forward current increases with decreasing electron beam diameter.

From the *I–V* curves shown in Fig. 2b, the open-circuit voltage, V_{OC}, across the probe contact measured at zero current was estimated to be about 1.5 V. This is much higher than the ~0.6 V typically found in commercial solar cells made of polycrystalline silicon [7]. It is likely that 1.5 V does not represent V_{OC} alone, but also includes the effects of induced charges present in the p-type Si due to electron-beam illumination. If the induced charges are mainly from secondary electron emission due to the high-energy incident electrons, net positive charges will be present on the sample's surfaces. These positive surface charges will shift the *I–V* curves upwards, resulting in an apparent high open voltage of V_{OC} = 1.5 V.

To measure the electron diffusion length in the sample, a 100 nm diameter electron beam was focused on various positions between the probe contact and sample (Fig. 3a), and *I–V* curves collected for each position. A 100 nm diameter electron beam was chosen because of the difficulty in accurately positioning electron beams of smaller diameter with condenser lens shift coils. The distance between the centers of the beam positions was about 50 nm, with position *c* centered on the probe contact. As the electron beam was moved closer to the probe contact (from *l* to *c*), EBICs increased in the manner shown in Fig. 3b. When the electron beam was directed at the probe alone (points *a* and *b*), the *I–V* curves were almost identical to that obtained without illumination (i.e., when the electron gun valve was closed). The *I–V* curves measured at positions *c* and *d* in reverse bias are conspicuous in that they are shaped differently to those measured at other positions in the sample (*e–l*) and do not obey the overall trend. This is because the ehps generated at positions *c* and *d* are still within the collecting region ($\Delta + L_n$) even at zero bias, as illustrated in Fig. 3a. Thus the reverse bias, which expands the depletion (and hence collecting) region, does not have a strong influence on the EBICs at these two points. A maximum I_{sc} of about 300 nA was obtained from electron beam positions *d* and *e*.

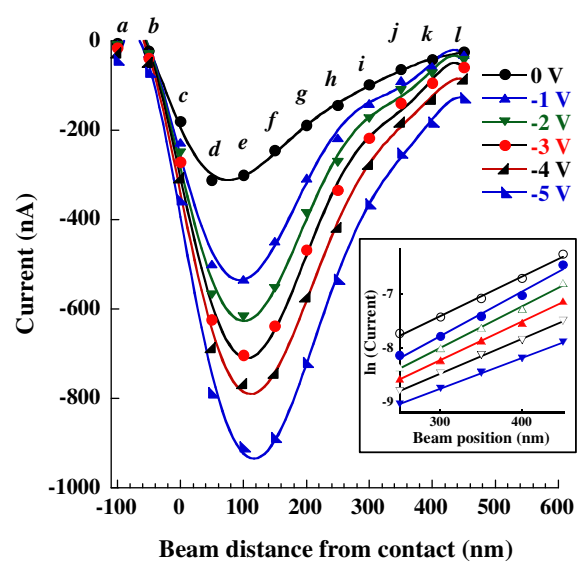

Fig. 4. EBIC dependence on the distance of the electron beam from the probe contact point with external biases of 0 (short circuit) to −5 V. Positive distances correspond to electron beams centered on the sample, and negative to those centered on the *W* probe. The inset shows a semi-log plot of curve tails from which the carrier diffusion length was extracted.

For a typical thermal-assisted field emission electron gun, the incident-beam current with the sample is of the order of a few nA for a nanometric probe. Thus, the measured I_{sc} indicates significant current amplification due to generation of multiple ehps in the illuminated region for each impinging 300 keV electron. By way of comparison it is worth noting that Houben et al. estimated that for each 200 keV incident electron, one ehp is generated per 10 nm of penetration depth in silicon [8].

The EBICs in Fig. 3b are plotted as a function of distance from the probe contact in Fig. 4 under various reverse bias conditions. As the electron beam is moved away from the contact, the EBIC decays exponentially. The plot minima shift away from the contact as the reverse bias increases due to the corresponding expansion of the depletion region.

Under steady-state conditions, the dependence of EBIC measured under reverse bias conditions on the distance from the probe contact, D, is given by

$$I \propto \exp(-D/L_n) \tag{1}$$

where I is the measured current at reverse bias. Using the above relationship, L_n was estimated from the slopes obtained in the inset of Fig. 4 to be about 150 ± 20 nm. This is much shorter than that reported for bulk p-type Si, which is typically a few microns [9]. This discrepancy can be explained by the fast surface recombination that occurs in thin TEM samples because the sample thickness is comparable to the carrier diffusion length. Measurement of the electric field distribution inside the sample, especially around the probe contact, is necessary to better understand the effects of surface recombination on carrier diffusion. It should be noted that lattice strain effects from the probe contact, as well as any contaminants on the *W* probe or in the p-type Si sample, including native oxide, were not considered in this study.

4. Summary and conclusion

We have measured EBICs *in situ* near the contact region between a *W* probe and a p-type Si sample in a TEM. The short-circuit current reached a maximum of about 300 nA for a 300 keV electron beam 100 nm in diameter. From EBIC decay curves, the electron diffusion length in the p-type Si was determined to be 150 ± 20 nm, which is shorter than that for bulk Si. The method provides a direct way to measure minority carrier diffusion lengths of semiconductor materials inside a TEM so that simultaneous electrical characterization can be carried out in conjunction with high-resolution structural analysis. The method also can be used to study the effects of electron-beam illumination during *in situ* TEM electrical characterization of nano-engineered materials, or potential mapping of semiconductors using *in situ* electron holography, for example.

Acknowledgement

The authors thank Kazuo Yamamoto for help preparing the W probe.

References

[1] Leamy HJ. Charge collection scanning electron microscopy. J Appl Phys 1982;53:R51–80.
[2] Berz F, Kuiken HK. Theory of life time measurements with the scanning electron microscope: steady state. Solid State Electron 1976;19:437–55.
[3] Sparrow TG, Valdrèg U. Application of scanning transmission electron microscopy to semiconductor devices. Philos Mag 1977;36:1517.
[4] Petroff PM, Logan RA, Savage A. Nonradiative recombination at dislocations in III–V compound semiconductors. Phys Rev Lett 1980;44:287–91.
[5] Cabanel C, Laval JY. Localization of the electrical activity of structural defects in polycrystalline silicon. J Appl Phys 1990;67:1425–32.
[6] Tanaka S, Tanaka H, Kawasaki T, Ichihashi M, Tanji T, Arafune K, Ohshita Y, Yamaguchi M. EBIC imaging using scanning transmission electron microscopy: experiment and analysis. J Mater Sci Mater Electron 2008;19:S324–7.
[7] Kerr MJ, Cuevas A, Sinton RA. Generalized analysis of quasi-steady-state and transient decay open circuit voltage measurements. J Appl Phys 2002;91:399–404.
[8] Houben L, Luysberg M, Brammer T. Illumination effects in holographic imaging of the electrostatic potential of defects and *pn* junctions in transmission electron microscopy. Phys Rev B 2004;70:165313.
[9] Ioannou DE, Dimitriadis CA. A SEM-EBIC minority-carrier diffusion-length measurement technique. IEEE Trans Electron Dev 1982;ED-29:445–50.